POLITECNICO
MILANO 1863

SCUOLA DI INGEGNERIA INDUSTRIALE
E DELL'INFORMAZIONE

Executive Summary of the Thesis

Investigation of Laguerre expansion basis for modelling of bridge aeroelastic forces

Laurea Magistrale in Mechanical Engineering - Ingegneria Meccanica

Author: Giacomo Bacci

Advisor: Prof. Tommaso Argentini (PoliMi)

Co-advisor: Prof. Ole Andre Øiseth (NTNU)

Academic year: 2021-2022

Introduction

In the process of designing long-span cable suspended bridges, wind-induced dynamic response is one of the major concerns. Wind action on cables, towers and girder can induce vibrations that can damage or weaken the structure. In recent years great progress has been done to develop models able to accurately reproduce the bridge dynamic response under wind action. However, simplified models are still helpful in preliminary design phases and to assess the reliability of the project.

The aim of this work is to develop an effective and easy-to-evaluate model for self-excited forces on bridge decks. The intention of the author is to investigate the feasibility of a variation from the work of Skyvulstad et al. [5], who approximated the unsteady forces with a Volterra expansion, parameterised with Laguerre expansion basis. In the present work, the Volterra expansion is stopped at the first order, and Laguerre orthonormal functions are used to parameterise the linear kernel.

The use of a parameterised model reduces the number of unknowns and the computational burden of the model. Moreover, these orthonormal functions are good filters for high-order noise and have an in-built negative exponential, which makes them suitable to approximate most mechanical systems' impulse response functions. In the present work, a training procedure is developed and tested on a simulated first order model and then on real wind tunnel data. The Laguerre model performances are then compared in time and frequency domain, with the rational functions model, often used to interpolate experimental data in wind engineering [3]. Finally, to check the applicability of the force prediction model, it is coupled with a complete girder section dynamical system and stability limits prediction is evaluated.

1. Orthonormal Functions Approximation

Any kind of continuous real function can be written as a linear combination of orthonormal functions from a complete set $\{g_l(\tau)\}$. It is interesting to express the unit-impulse response of a linear system, from the input m to the output n, as an infinite summation of orthonormal functions $h_{nm}(t) = \sum_{l=0}^{\infty} c_l^{nm} g_l(t)$. Here the $g_l(t)$ is the function of order l, which is multiplied by the relative coefficient c_l^{nm}.

However, thanks to the properties of complete

orthonormal sets, if the system has all poles strictly on the left-half complex plane, the impulse response function can be approximated with a finite summation, as in Equation (1), with increasing accuracy with the number of terms considered L. Similarly, also the transfer function can be written as in Equation (2), where $G_l(z)$ is the z-transform of $g_l(t)$.

$$h_{nm}(t) = \sum_{l=0}^{L} c_l^{nm} g_l(t) \tag{1}$$

$$H_{nm}(z) = \sum_{l=0}^{L} c_l^{nm} G_l(z) \tag{2}$$

The expression of the set of discrete Laguerre orthonormal functions considered in the present work is shown in Equation (3). The shape of these functions depends on two parameters: the decay factor α, and the filter order l. Laguerre functions for different orders are shown in Figure 1. The Fourier transform of the set is then shown in Equation (4).

$$g_n(k) = \alpha^{\frac{k-n}{2}}(1-\alpha)^{1/2} \sum_{i=0}^{n}(-1)^i \binom{k}{i}\binom{n}{i}\alpha^{n-i}(1-\alpha)^i \tag{3}$$

$$G_n(z) = \left(\frac{\sqrt{\alpha}-z^{-1}}{1-\sqrt{\alpha}z^{-1}}\right)^n \left(\frac{\sqrt{1-\alpha}}{1-\sqrt{\alpha}z^{-1}}\right) \tag{4}$$

From the impulse response function it can be expressed the self-excited force relative to the specific input, as in Equation (5).

$$F_n(n) = \sum_{k=0}^{M}\sum_{l=0}^{L} c_l^{nv} g_l(k) v(n-k) \tag{5}$$

Where $v(n)$ is the input motion convoluted with the sum of filters, evaluated over the memory length M.

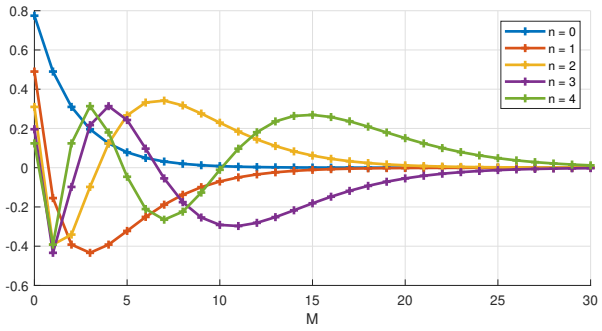

Figure 1: Laguerre functions $g_n[k]$ with $n \in [0, 1, \ldots 4]$, $\alpha = 0.4$.

The expression in Equation (5) can be expressed in matrix form as $\boldsymbol{F}_n = \boldsymbol{S}_v \boldsymbol{c}^{nv}$. Where $\boldsymbol{S}_v$ is the regression matrix containing the Laguerre filters convoluted with the input. The model training performances are improved by constructing this matrix with the recursive relation in Equation (6). Thanks to this expression, the memory length M is not a parameter of the model anymore, and the effective memory is determined only by the longest stretching filter.

$$\begin{aligned} s_0[k] &= \sqrt{\alpha}s_0[k-1] + \sqrt{1-\alpha}v[k], s_0[0] = 0 \\ s_l[k] &= \sqrt{\alpha}s_l[k-1] + \sqrt{\alpha}s_{l-1}[k] + \\ &\quad - s_{l-1}[k-1],\ l = 1, \ldots L, \quad s_l[0] = 0 \end{aligned} \tag{6}$$

The vector of unknown coefficients is then determined solving the least-squares problem as shown in Equation (7).

$$\boldsymbol{c}^{nv} = (\boldsymbol{S}_v^T \boldsymbol{S}_v)^{-1} \boldsymbol{S}_v^T \boldsymbol{F}_n \tag{7}$$

Once the model is trained as shown, the output can be foreseen for any input using Equation (5). The here exposed training procedure can be calibrated for optimal model parameters. In Figures 2 and 3 it is shown the impulse response function approximation of a simulated first order system with the Laguerre model for different values of model parameters.

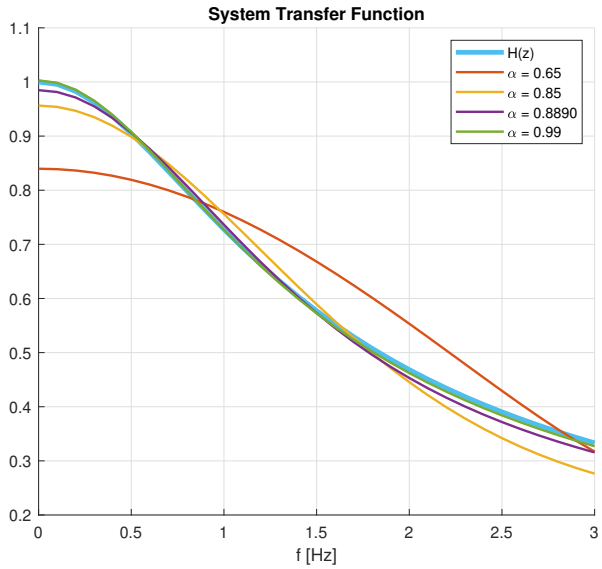

Figure 2: Transfer function approximation for different decay factors. $L = 3$.

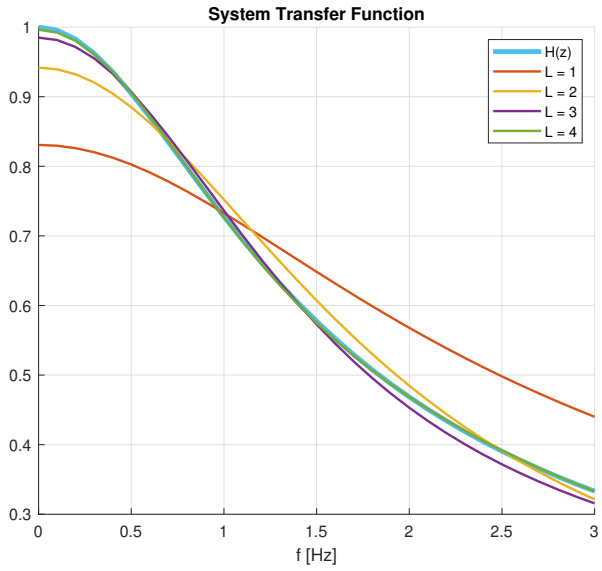

Figure 3: Transfer function approximation for different numbers of filters considered. $\alpha = 0.889$.

2. Langenuen Experimental Campaign

The identified model is been tested on real wind tunnel data. The used data have been collected during an experimental campaign in the wind tunnel of the Norwegian University of Science and Technology (NTNU) [1]. A special forced motion rig has been used, shown in Figure 5, capable of forcing the girder model in almost any desired motion in the wind flow.

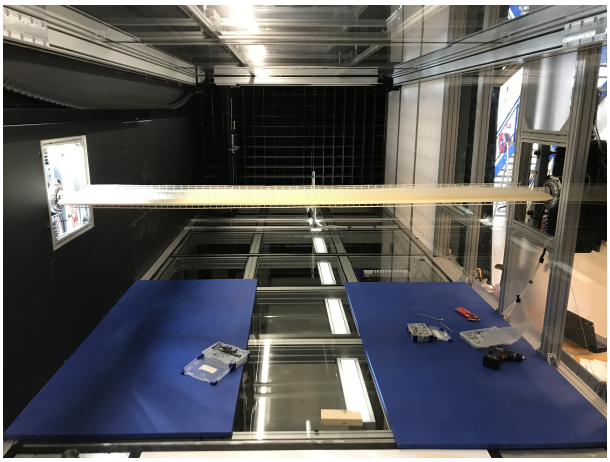

Figure 5: NTNU test vibration rig: experiment preparation.

Thanks to the very light computational burden of the presented model, the identification procedure has been calibrated with a trial and error procedure, comparing the predicted time history with the measured data for different values of the model parameters. An example of forced input motion time history and measured aerodynamic forces can be seen in Figure 4. The time history comparison has been carried out with the *Compmet.m* Matlab toolbox by Kavrakov et al.[2]. Which compares two time histories calculating goodness of fit metrics. The metrics selected for this work were the Phase metric M_Φ, the Peak metric M_p and the Magnitude Warped metric M_{mw}. The M_Φ metric measures the capability of the model to capture the fluid memory effect. The M_p metric measures how well the model fits the peak value of the self-excited forces, which is an important design criterion for long span bridges. The M_{mw} metric measures the differences of magnitude in a localized manner, independently from the phase shift between the two compared signals.
The selected optimal parameter values are $\alpha = 0.6$ and $L = 3$.
The performances of the model have been checked to be independent of the geometry of the girder. This was done by evaluating the goodness of the prediction in time domain for different geometries tested. In Figure 7 are shown the goodness of fit metrics for different sections tested. Apart from little variations in the peak

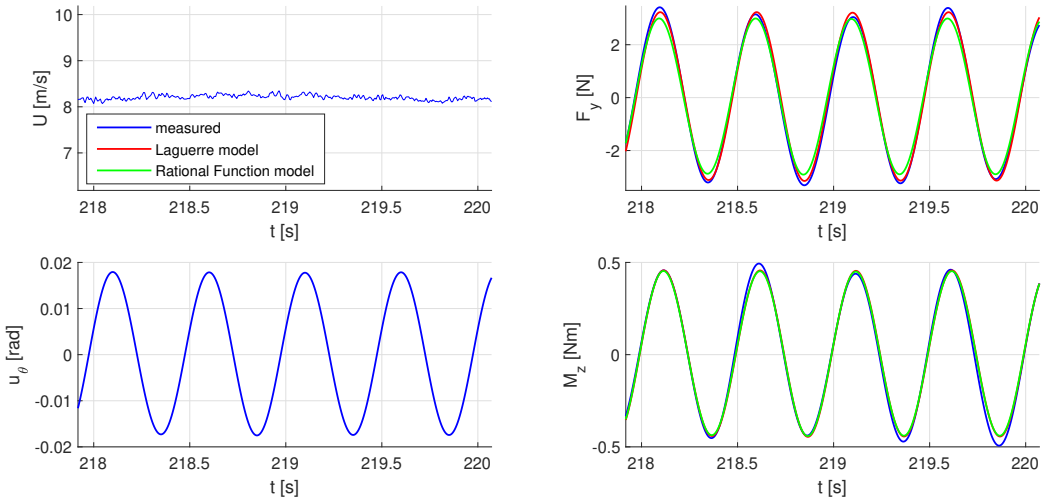

Figure 4: Particular of time histories. Input torsional motion at 2.0Hz. Section LN21-5200. Comparison between measured and modelled forces with rational functions and Laguerre model.

metric for the lift force, it can be concluded that in general, the model performances are independent of minor changes in the girder geometry.
The model performances have been also evaluated in frequency domain, comparing the transfer functions modelled with Equation (2) with the ones determined with experimental aerodynamic derivatives. The results are shown in Figures 8 and 9. As shown, the modelled transfer functions module is always included in the band of $\pm 15\%$ of the experimental one. The phase is always enclosed in the band of $\pm 5deg$, apart from the transfer function for the torque because of vertical motion. This is a consequence of the model not being able to correctly identify the aerodynamic derivative A_1^* linking the vertical speed to the torsion, as shown also in Figure 11. The identified Laguerre model has been also compared to a well-established model for experimental data interpolation: the rational functions model. The two models are compared in time domain calculating the metrics between the modelled forces and the measured forces. The results are shown in Figures 4 and 10. It is proved that the two models perform in general similarly in time domain, especially for the module prediction. For a deeper analysis, they have been compared also in frequency domain comparing their prediction for the aerodynamic derivatives. The results are reported in Figures 11 to 14. From this latter analysis, it is highlighted how the two models do not perform equally for the whole tested frequency range. The bigger discrepancy is shown, as said, for the A_1^* prediction for low excitation frequency.

3. Girder Section Dynamic Simulation

Once the Laguerre model has been trained and proved to perform well for wind-induced forces identification, it has been coupled with a simulated two degrees of freedom girder section dynamical system. With this aim a state-space representation for the Laguerre expansion model has been formulated. This is achieved by writing in matrix form the recursive relation in Equation (6), obtaining Equation (8a).

$$\boldsymbol{S}_v(k+1) = \boldsymbol{A}_L \boldsymbol{S}_v(k) + \boldsymbol{B}_L v(k+1) \tag{8a}$$

$$F_n(k) = \boldsymbol{c}_{nv} \boldsymbol{S}_v(k) \tag{8b}$$

$$\boldsymbol{A}_L = \begin{bmatrix} \sqrt{\alpha} & 0 & 0 & \dots & 0 \\ \alpha - 1 & \sqrt{\alpha} & 0 & \dots & 0 \\ \sqrt{\alpha}(\alpha-1) & \alpha - 1 & \sqrt{\alpha} & \dots & 0 \\ \vdots & & & \ddots & 0 \\ (\sqrt{\alpha})^{n-2}(\alpha-1) & & & & \sqrt{\alpha} \end{bmatrix} \tag{9}$$

$$\boldsymbol{B}_L = \sqrt{1-\alpha} \begin{bmatrix} 1 \\ \sqrt{\alpha} \\ (\sqrt{\alpha})^2 \\ \vdots \\ (\sqrt{\alpha})^{n-1} \end{bmatrix} \tag{10}$$

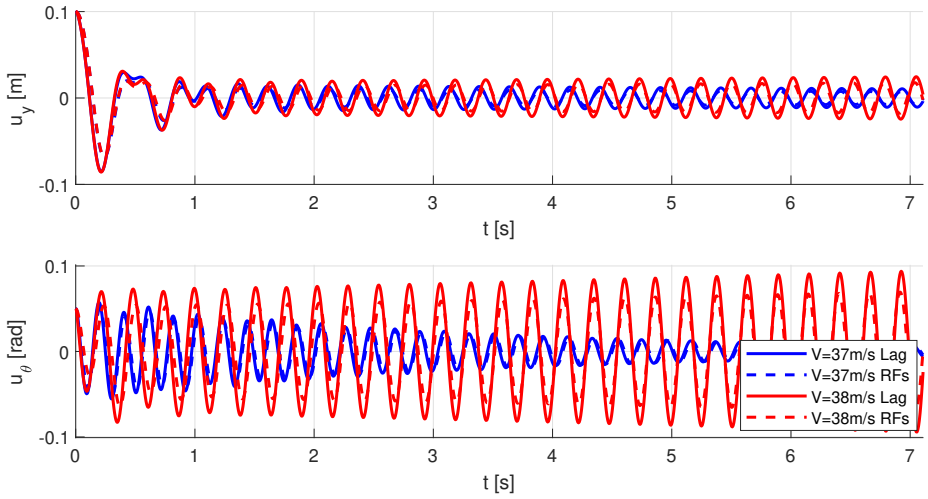

Figure 6: The coupled dynamic model has been simulated for different speeds until instability was observed. Flutter speed $V = 37.6m/s$.

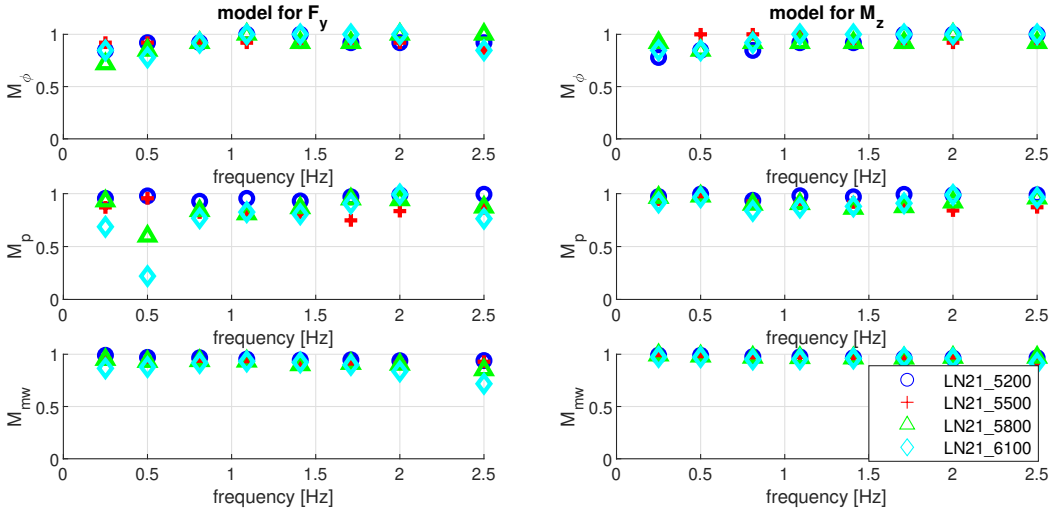

Figure 7: Goodness of fit metrics for different sections tested. Input torsional motion. Laguerre model prediction compared with measured forces.

Here the input motion time history is $\boldsymbol{v}$, leading to the aerodynamic force $\boldsymbol{F}_n$. The vector $\boldsymbol{c}_{nv}$ is the vector of identified Laguerre coefficients corresponding to the transfer function between the input $\boldsymbol{v}$ and the output force $\boldsymbol{F}_n$.
To be inserted in a two degrees of freedom aerodynamic model, the system in Equation (8) needs to be expanded to consider all the possible transfer functions as shown in Equation (11).

$$\boldsymbol{F}(k) = \begin{bmatrix} \boldsymbol{c}_{yy} & \boldsymbol{c}_{y\theta} & \boldsymbol{0} & \boldsymbol{0} \\ \boldsymbol{0} & \boldsymbol{0} & \boldsymbol{c}_{\theta y} & \boldsymbol{c}_{\theta\theta} \end{bmatrix} \begin{bmatrix} \boldsymbol{S}_y(k) \\ \boldsymbol{S}_\theta(k) \\ \boldsymbol{S}_y(k) \\ \boldsymbol{S}_\theta(k) \end{bmatrix} \tag{11}$$
$$= \boldsymbol{C}\hat{\boldsymbol{S}}(k)$$

The Laguerre state-space model is then inserted in the equations of motion of the deck's dynamical system.
The continuous time equations of motion of a two degrees of freedom deck section in Equation (12) are rewritten in state-space form in Equation (13). Where the state vector $\boldsymbol{X} = [y(t), \theta(t), \dot{y}(t), \dot{\theta}(t)]^T$ is defined, containing displacement and velocity time histories in the vertical and torsional directions. Since the Laguerre model has been developed in discrete time, the system matrices $\boldsymbol{A}_c$ and $\boldsymbol{B}_c$ are discretised with

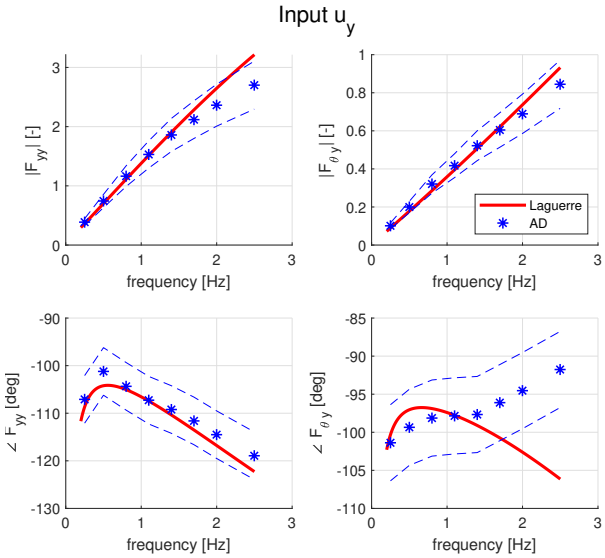

Figure 8: Module and phase of transfer functions linking the vertical motion to lift and torque.

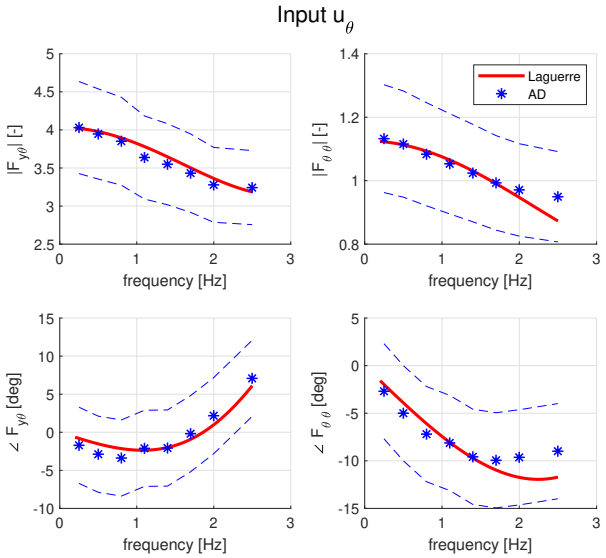

Figure 9: Module and phase of transfer functions linking the torsional motion to lift and torque.

the relations in Equation (14).

$$\begin{bmatrix} m_y & 0 \\ 0 & J \end{bmatrix} \begin{bmatrix} \ddot{y}(t) \\ \ddot{\theta}(t) \end{bmatrix} + \begin{bmatrix} r_y & 0 \\ 0 & r_\theta \end{bmatrix} \begin{bmatrix} \dot{y}(t) \\ \dot{\theta}(t) \end{bmatrix} + + \begin{bmatrix} k_y & 0 \\ 0 & k_\theta \end{bmatrix} \begin{bmatrix} y(t) \\ \theta(t) \end{bmatrix} = \begin{bmatrix} F_y(t) \\ F_\theta(t) \end{bmatrix} = \boldsymbol{F}(t) \tag{12}$$

$$\begin{aligned} \dot{\boldsymbol{X}}(t) &= \begin{bmatrix} \boldsymbol{0} & \boldsymbol{I} \\ -\boldsymbol{M}^{-1}\boldsymbol{K} & -\boldsymbol{M}^{-1}\boldsymbol{R} \end{bmatrix} \boldsymbol{X}(t) + \\ &+ \begin{bmatrix} \boldsymbol{0} \\ \boldsymbol{M}^{-1} \end{bmatrix} \boldsymbol{F}(t) \\ &= \boldsymbol{A}_c \boldsymbol{X}(t) + \boldsymbol{B}_c \boldsymbol{F}(t) \end{aligned} \tag{13}$$

$$\boldsymbol{A} = e^{\boldsymbol{A}_c \Delta t}, \ \boldsymbol{B} = [\boldsymbol{A} - \boldsymbol{I}] \boldsymbol{A}_c^{-1} \boldsymbol{B}_c \tag{14}$$

Expanding the Laguerre matrices $\boldsymbol{A}_L$, $\boldsymbol{B}_L$ as shown in Equation (15), the complete system state space model is obtained as in Equation (16).

$$\begin{aligned} \hat{\boldsymbol{A}}_L &= \begin{bmatrix} \boldsymbol{A}_L & & & \\ & \boldsymbol{A}_L & & \\ & & \boldsymbol{A}_L & \\ & & & \boldsymbol{A}_L \end{bmatrix} \\ \hat{\boldsymbol{B}}_L &= \begin{bmatrix} \boldsymbol{B}_L & \boldsymbol{0} \\ \boldsymbol{0} & \boldsymbol{B}_L \\ \boldsymbol{B}_L & \boldsymbol{0} \\ \boldsymbol{0} & \boldsymbol{B}_L \end{bmatrix} \end{aligned} \tag{15}$$

$$\boldsymbol{X}(k+1) = \boldsymbol{A}\boldsymbol{X}(k) + \boldsymbol{B}\boldsymbol{C}\hat{\boldsymbol{S}}(k) \tag{16a}$$

$$\hat{\boldsymbol{S}}(k+1) = \hat{\boldsymbol{A}}_L \hat{\boldsymbol{S}}(k) + \begin{bmatrix} \hat{\boldsymbol{B}}_L & \boldsymbol{0} \end{bmatrix} \boldsymbol{X}(k+1) \tag{16b}$$

Using the complete state-space model, time simulations have been carried out for different wind speeds. The wind speed was increased until the system showed unstable motion because of the coupling between the two degrees of freedom. The transition to unstable behaviour can be seen from the time histories in Figure 6. When the wind speed exceeds $V = 37.6 m/s$ the motion starts to diverge. This kind of instability, in bridge aerodynamics, is called flutter instability and the corresponding wind speed is the flutter critical speed. Flutter instability is one of the main issues in suspended bridges design and occurs when the high wind speed causes the bridge first torsional frequency of vibration to decrease and get nearer to the vertical one, as can be seen from the simulation results in Figure 16. This causes the real part of the corresponding eigenvalues to become positive and hence gives rise to instability. The value of flutter critical speed identified with the Laguerre model has been compared with the value found with a state-space model constructed with rational function identification method for self-excited forces [4]. The data used for the girder two degrees of freedom model are shown in Table 1.

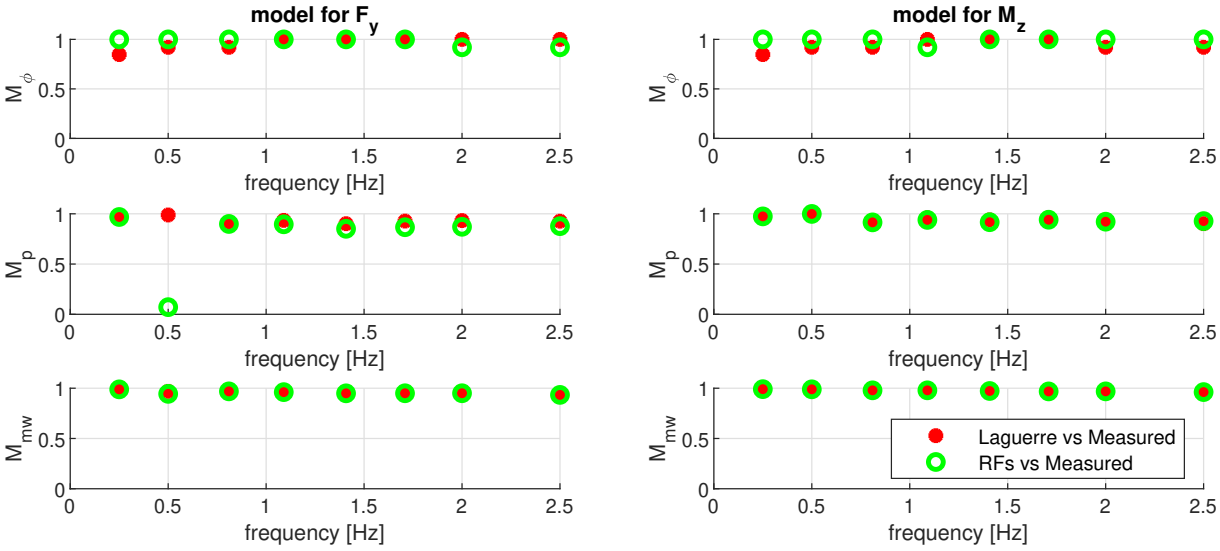

Figure 10: Goodness of fit metrics comparing measured forces and modelled forces for torsional input. Self-excited forces are modelled with Laguerre model and rational functions model.

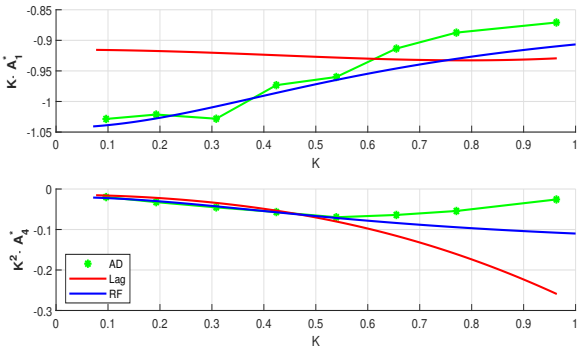

Figure 11: Fitting of aerodynamic derivatives relative to torque because of vertical motion.

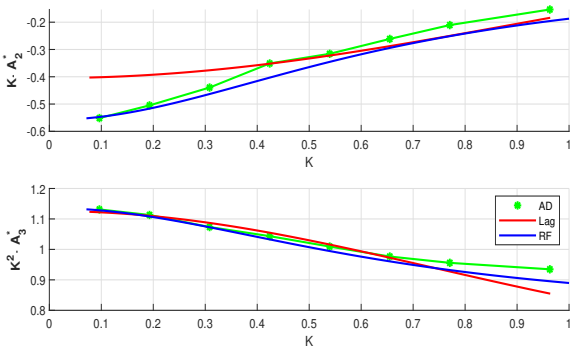

Figure 12: Fitting of aerodynamic derivatives relative to torque because of torsional motion.

Width	$0.50\,m$	f_v	$2Hz$
Length	$2.68\,m$	f_t	$5Hz$
m	$15\,Kg/m$	ρ_{air}	$1.19\,Kg/m^3$
J	$0.6Kgm^2/m$	ξ	3 ‰
$V \in [17, 18, 19, ..., 40]$ m/s			

Table 1: Simulation data for 2 Dof aeroelastic deck model.

For each wind speed the eigenvalues of the system $\lambda_{1,2}$, identified with the two models, are plotted in Figure 15. It is visible that towards the last wind speeds the system becomes unstable. This is confirmed by the torsional damping coefficient that becomes negative as the wind speed increases, as shown in Figure 16. The flutter critical speed identified with the two models is in both cases around $V = 37.6m/s$.

4. Conclusions

In the present work the feasibility of a linear Laguerre expansion model for the approximation of wind-induced forces on suspended bridge decks has been explored. This work originated from the work of Skyvulstad et al. [5], who used a parameterised Volterra model for non-linear approximation of drag force. The intention of the author was to develop a model stopping the Volterra expansion at the first order and express the linear kernel with parametric Laguerre functions. This aim was achieved and an effective parametric linear model has been obtained and

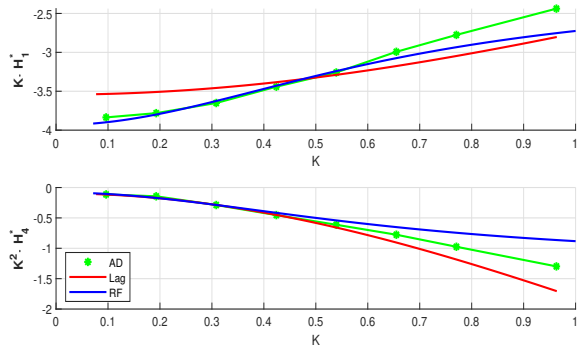

Figure 13: Fitting of aerodynamic derivatives relative to lift because of vertical motion.

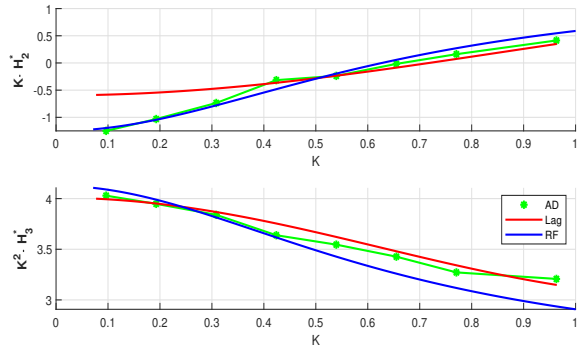

Figure 14: Fitting of aerodynamic derivatives relative to lift because of torsional motion.

a training procedure was developed.
The effectiveness of the model was verified on real data from wind tunnel experiments. In time domain the forces were well reconstructed and in frequency domain the model behaved well for most of the training frequencies.
The model performances have also been proved to be independent of minor changes in the section geometry as a variety of experimental data on different girder geometries was available.
Thanks to the limited computational burden of the model, an experimental investigation for optimal calibration of the model parameters was carried out. Once the model was trained with optimal parameters, its performances have been compared with the rational functions model. The training computational burden is comparable and the performance of the two models is very similar in time domain, the differences have been highlighted by analysing the frequency domain predictions.
The Laguerre expansion model for aerodynamic forces prediction is then coupled with a simulated two degrees of freedom (2Dof) girder dynamic model. The flutter critical speed is then investigated. The results obtained are compared with the one calculated using the rational functions as force prediction model in the dynamic system. It can be highlighted how in practice, the two models perform in a very similar way (see Figures 15 and 16) determining the same instability points for the system.

The presented Laguerre expansion model gave interesting results and has room for further improvement. In the model definition could be added two feed-through terms relative to speed and displacement to improve the impulse response approximation. The absence of these terms is one of the main reasons for the small discrepancies with the rational function model.
Furthermore, the training procedure could be further developed training a different set of parameters for each transfer function in the system, while in the present work only one value for α and L was used for the whole identification.
A further alternative which is worth testing would be to reformulate the model starting from a continuous time formulation of Laguerre filters instead of a discrete one. Finally, it would be interesting to investigate the eventual differences in performances using white noise as training data instead of a single harmonic motion.

References

[1] Jens Petter Bergerud and Håvard Morvik Torød. Shape optimization of an aluminium girder for a long-span suspension bridge. Master's thesis, NTNU, 2021.

[2] Igor Kavrakov, Ahsan Kareem, and Guido Morgenthal. Comparison Metrics for Time-Histories: Application to Bridge Aerodynamics. *Journal of Engineering Mechanics*, 146(9):04020093, 2020.

[3] Ole Øiseth, Anders Rönnquist, and Ragnar Sigbjörnsson. Time domain modeling of self-excited aerodynamic forces for cable-supported bridges: A comparative study. *Computers and Structures*, 89(13-14):1306–1322, 2011.

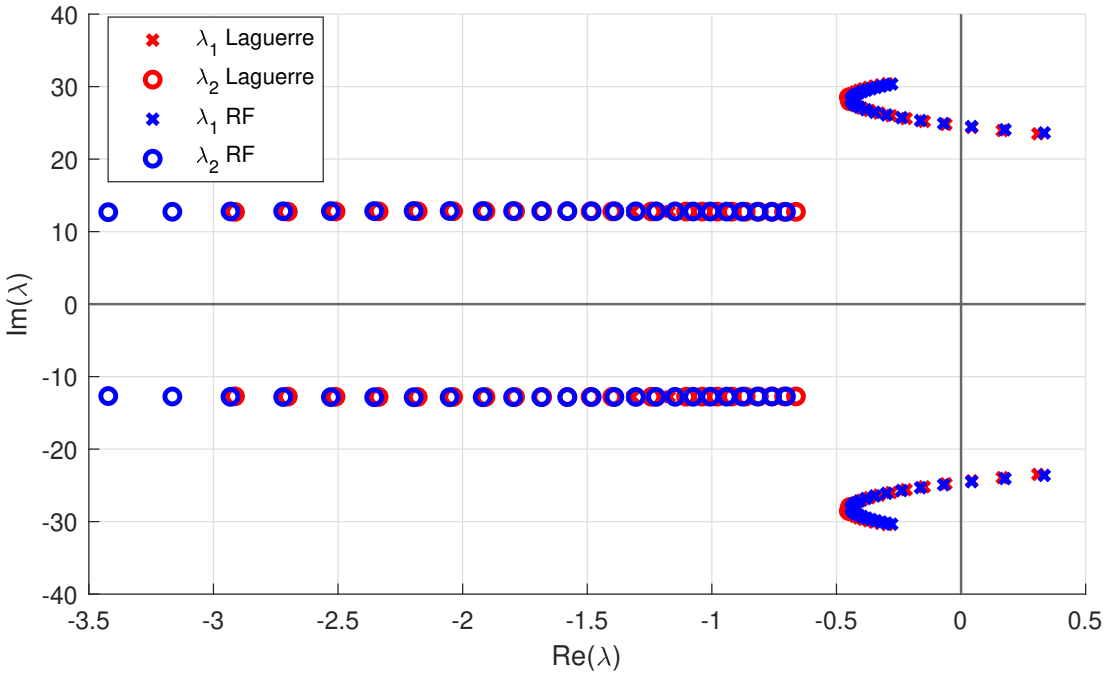

Figure 15: Continuous time 2 Dof system eigenvalues corresponding to first vertical and torsional vibration modes in function of wind speed.

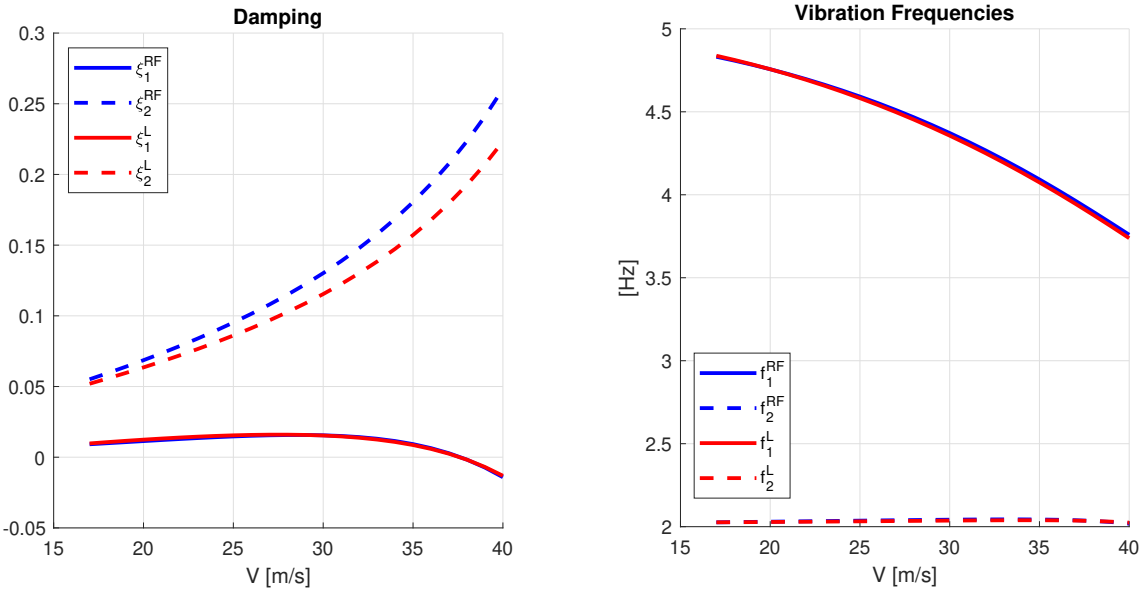

Figure 16: 2 Dof system first vertical and torsional damping coefficients and vibration frequencies in function of wind speed.

[4] Ole Øiseth, Anders Rönnquist, and Ragnar Sigbjörnsson. Finite element formulation of the self-excited forces for time-domain assessment of wind-induced dynamic response and flutter stability limit of cable-supported bridges. *Finite Elements in Analysis and Design*, 50:173–183, 2012.

[5] Henrik Skyvulstad, Øyvind W. Petersen, Tommaso Argentini, Alberto Zasso, and Ole Øiseth. The use of a Laguerrian expansion basis as Volterra kernels for the efficient modeling of nonlinear self-excited forces on bridge decks. *Journal of Wind Engineering and Industrial Aerodynamics*, 219(February), 2021.